AIP | Review of Scientific Instruments

Pulse shape measurements using single shot-frequency resolved optical gating for high energy (80 J) short pulse (600 fs) lasera)

S. Palaniyappan, R. C. Shah, R. Johnson, T. Shimada, D. C. Gautier, S. Letzring, D. Jung, R. Hörlein, D. T. Offermann, J. C. Fernández, and B. M. Hegelich

Citation: Review of Scientific Instruments **81**, 10E103 (2010); doi: 10.1063/1.3464258
View online: http://dx.doi.org/10.1063/1.3464258
View Table of Contents: http://scitation.aip.org/content/aip/journal/rsi/81/10?ver=pdfcov
Published by the AIP Publishing

Pulse shape measurements using single shot-frequency resolved optical gating for high energy (80 J) short pulse (600 fs) laser[a)]

S. Palaniyappan,[1,b)] R. C. Shah,[1,2] R. Johnson,[1] T. Shimada,[1] D. C. Gautier,[1] S. Letzring,[1] D. Jung,[1,2] R. Hörlein,[2] D. T. Offermann,[1] J. C. Fernández,[1] and B. M. Hegelich[1,2]
[1]*Los Alamos National Laboratory, Los Alamos, New Mexico 87544, USA*
[2]*Ludwig-Maximilians-Universität München, Munich 85748, Germany*

(Presented 19 May 2010; received 14 May 2010; accepted 1 June 2010; published online 4 October 2010)

Relevant to laser based electron/ion accelerations, a single shot second harmonic generation frequency resolved optical gating (FROG) system has been developed to characterize laser pulses (80 J, ~600 fs) incident on and transmitted through nanofoil targets, employing relay imaging, spatial filter, and partially coated glass substrates to reduce spatial nonuniformity and B-integral. The device can be completely aligned without using a pulsed laser source. Variations of incident pulse shape were measured from durations of 613 fs (nearly symmetric shape) to 571 fs (asymmetric shape with pre- or postpulse). The FROG measurements are consistent with independent spectral and autocorrelation measurements. © *2010 American Institute of Physics.* [doi:10.1063/1.3464258]

I. INTRODUCTION

Acceleration of electrons and ions to GeV energies by laser-plasma interactions could produce unique subpicosecond electron, ion, and x-ray bunches with reduced footprint and cost over conventional sources.[1,2] Recently, it was shown numerically that acceleration of ions to ~GeV energies could be achieved via breakout-after-burner mechanism[3] in laser-nanofoil interactions at $>10^{20}$ W/cm^2. Numerical studies[4] have also shown that when an intense laser ($\sim 10^{20}$ W/cm^2) interacts with an intact nanofoil, the relativistic increase of electron mass reduces the plasma frequency and causes self-induced transparency. The transmitted pulse is temporally shortened and has a faster rise time, which, in turn, can be used to accelerate electrons and ions efficiently in a second nanofoil.[5] Also, high intensity lasers ($\sim 10^{20}$ W/cm^2) are susceptible to pulse shape variations, which can have a significant impact on the laser-nanofoil interactions. Thus, it is of interest to characterize such incident laser pulse shapes and its effects on such interactions along with the transmitted laser pulse shapes.

There are two well known techniques for characterization of such laser pulses, viz., spectral phase interferometry for direct electric field reconstruction (SPIDER)[6]) and frequency resolved optical gating (FROG).[7,8] While both techniques can be used to measure short pulses, for long pulses the FROG is more desirable since SPIDER would require a spectrometer with very high resolution and an optical element with a huge amount of chromatic dispersion. Thus, we have developed a single shot second harmonic generation (SHG) FROG to characterize the laser pulses from the Trident laser system (80 J, ~600 fs, 1.054 μm, ~1 shot/h, $>10^{20}$ W/cm^2, and $\sim 10^{-10}$ contrast) in Los Alamos National Laboratories for ultraintense laser-nanofoil interactions. Such experiments are enabled by ultrahigh contrast ($\sim 10^{-10}$), removing long time ASE.[9] The FROG measurements can be naturally verified with independent spectral and autocorrelation measurements. Implementing a single shot SHG-FROG pulse characterization system for a high energy, low rep rate laser is not straightforward due to issues such as optical damage, nonlinear spatiotemporal modification of the pulse, spatial nonuniformity of input beam, diffraction effects, low rep rate, and the need to align the device without the actual laser. The developed system is engineered to address these issues in order to characterize the intense laser pulses.

The SHG-FROG measures the second harmonic autocorrelation signal of a laser pulse with its own replica and spectrally resolves it at all time delays to obtain a FROG trace, from which the pulse information is retrieved using an iterative two-dimensional phase retrieval algorithm. In a single shot SHG-FROG, the autocorrelation signal is obtained by mixing a pulse with its replica inside a nonlinear crystal in a cross-beam configuration, thus mapping space to time delay between two pulses. Grating-eliminated no-nonsense observation of ultrafast incident laser light E-fields (GRENOUILLE) is a well known fairly simple single shot SHG-FROG device, which uses a Fresnel biprism to split the beam into two halves and mix them in a cross-beam configuration inside a thick nonlinear crystal using the crystal both as a nonlinear medium and an imaging spectrometer. For our application, typical pulse widths and spectral bandwidths could change anywhere from ~600 fs and ~3 nm (incident) to ~300 fs and ~6 nm (transmitted) and characterizing such pulses would require a minimum spectral and temporal resolutions on the order of 0.1 nm (incident) and ~30 fs (transmitted), respectively, due to reciprocal Fourier transform

[a)]Contributed paper, published as part of the Proceedings of the 18th Topical Conference on High-Temperature Plasma Diagnostics, Wildwood, New Jersey, May 2010.
[b)]Author to whom correspondence should be addressed. Electronic mail: sasi@lanl.gov.

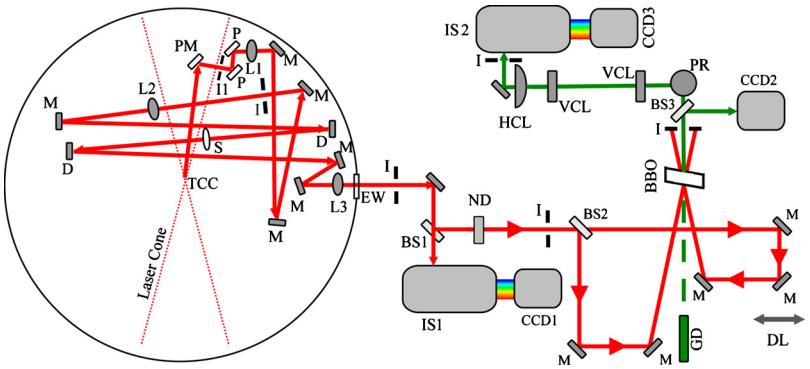

FIG. 1. (Color online) Layout of the laser pick-off scheme and single shot SHG-FROG system. TCC, target chamber center; PM, pick-off mirror; P, partially coated mirror; L1, collimating lens; D, dielectric mirror; L2 and L3, imaging lenses; S, spatial filter; I1 and I, iris; M, silver mirror; EW, exit window; BS1, 90/10 beam splitter; IS1 and IS2, imaging spectrometer; CCD1, CCD for spectrum; ND, neutral density filter; BS2, 50/50 beam splitter; GD, green laser diode; DL, adjustable optical delay; BBO, BBO crystal; BS3, 90/10 beam splitter; CCD2, CCD for autocorrelation; PR, periscope; VCL, vertical cylindrical lens; HCL, horizontal cylindrical lens; and CCD3, CCD for FROG.

constraint.[8] The developed system allows independent control and flexibility over mixing angle, crystal thickness, alignment, temporal, and spectral resolutions. In this paper, we present a single shot SHG-FROG system developed to characterize the variations in the incident intense laser pulse shapes. We also discuss the use of principal component generalized projection algorithm (PCGPA) to retrieve the pulse information from the measured FROG trace. Finally, we show the consistency of the FROG measurements with independent spectral and autocorrelation measurements. The observed laser pulse shortening and shaping in the transmitted laser pulses through nanofoils using the same SHG-FROG system will be discussed in separate publication.[4]

II. FROG SETUP

Figure 1 shows the layout of the laser pick-off scheme and the single shot SHG-FROG system that has been developed. The final amplified laser pulse from Trident laser system (20 cm diameter) is focused at the center of the target chamber center (TCC) by an f/#3 off-axis parabola to a spot size of 7 μm to create laser intensities around 10^{20} W/cm^2. A small (2.5 cm diameter), high damage threshold dielectric mirror (PM) at 47 cm away from TCC and 6.5° away from the center of the beam samples the diverging laser beam after the focus. The small pick-off mirror allows additional diagnostics to be positioned in the downstream and also provides spatially uniform input beam necessary for the single shot SHG-FROG. An independent autocorrelation measurement by collecting the full 20 cm beam shows a 5% pulse width fluctuation across the beam, which suggests that the FROG results from a small portion of the beam are representative of the full beam. At the pick-off mirror, the energy density in the diverging laser beam is calculated to be ~300 mJ/cm^2. The beam is apertured to 5 mm in size (59 mJ) using iris I1 and then successively reflected from two glass substrates (P) at 45° to attenuate the energy by approximately a 100-fold to 590 μJ. The laser pulse travels through ~2 cm of fused silica material (lenses L1, L2, and target chamber exit window) to reach the BBO crystal outside the target chamber, which gives a B-integral of 0.06, well below unity at which nonlinear effects will start to modify the spatiotemporal characteristics of the pulse.[10] The two glass substrates (P), coated with gold on their lower half surfaces (Bayview Optics), stand on a vertical translation stage which can be moved up to have the gold surfaces reflect the beam for alignment. A spherical lens with a focal length of 75 cm (L1) collimates the sampled diverging beam. After collimation, the beam is image relayed a distance of 8 m from the lens L1 to the BBO crystal using spherical lenses L2 and L3 with focal length of 2 m. From the lens L1, the beam propagates 6 m inside and 2 m outside the target chamber before it gets imaged onto the BBO crystal so as to keep the focus of the lens L2 inside the vacuum chamber. A spatial filter (S) with an aperture size of 1 mm (size of Airy disk formed by lens L2) is used at the focus of the lens L2 to reduce spatial nonuniformities.

Outside the target chamber, a 90/10 beam splitter (BS1) sends the transmitted 10% beam (59 μJ) to the imaging spectrometer IS1 (SureSpectrum 250is, Bruker Optics) and to the CCD1 (Grasshopper, Point Grey) for spectral measurement of the laser pulse. The imaging spectrometer IS1 had a spectral resolution of 0.25 nm with a 1200 lines/mm grating, blazed at 500 nm, and the entrance slit at 100 μm. The 90% reflected beam (531 μJ) from the beam splitter BS1 is attenuated by a neutral density (ND) filter by 70% (159 μJ) before it is further split into two beams by a 50/50 beam splitter (BS2). These two beams are mixed in a 500 μm thick BBO crystal (type I phase matching at 23°) at an external angle of 17° to produce second harmonic autocorrelation signal. For a 500 fs pulse, ~2 cm of fused silica (lenses L1, L2, and target chamber exit window) and 500 μm thick BBO crystal would stretch the input pulse by less than 1 fs due to group delay dispersion, which is negligible. The size of the input beam (D_{beam}=5 mm) and the half-mixing angle (φ=5.1°) inside the BBO crystal limits the longest pulse that can be measured with this setup to roughly 1.5 ps ($D_{beam} \tan \phi/c$). The smallest temporal feature that can be measured by this setup is limited by the phase matching bandwidth of the BBO crystal, which is 33 nm for our case, corresponding to a temporal feature of roughly 50 fs. The input fundamental beam is polarized along the horizontal direction at the BBO crystal and the doubled autocorrelation signal is polarized vertically along the extraordinary axis of the BBO crystal, thus the beam walks-off orthogonal to the time information inside the crystal.

The autocorrelation signal is then split in by a 90/10 beam splitter (BS3). The 10% reflected autocorrelation signal is captured by the CCD2 (Grasshopper, Point Grey) and the 90% transmitted autocorrelation signal is imaged on to the entrance slit of the imaging spectrometer IS2 (SureSpectrum 250is, Bruker Optics) along the temporal dimension and focused along the spatial dimension through a combination of cylindrical lenses to obtain the FROG trace. After the beam

splitter BS3, the periscope (PR) rotates the transmitted autocorrelation signal by 90°, which brings the temporal dimension along the vertical direction and the spatial dimension along the horizontal direction. Two vertical cylindrical lenses (VCLs) with focal lengths of 30 cm image the back plane of the BBO crystal on to the entrance slit of the imaging spectrometer IS2 along the temporal dimension. The distance between the two vertical cylindrical lenses is kept at a quarter of the 2f distance for the conventional 4f imaging system to reduce image vignetting. A horizontal cylindrical lens with a focal length of 20 cm along the spatial dimension is kept at ~15 cm away from the entrance slit of IS2 to loosely focus the autocorrelation signal on to the spectrometer. The imaging spectrometer IS2 had a spectral resolution of 0.1 nm with a 1200 lines/mm grating, blazed at 500 nm, and the entrance slit at 40 μm. The FROG trace is captured by water cooled, 12-bit CCD camera (Photometrics-CH250) with a chip size of 10×10 mm^2 and "512×512" arrays of pixels. The measured FROG trace has a spectral delay of 0.05 nm/pixel and temporal delay of 9.65 fs/pixel.

Using the optical parametric chirped pulse amplification front end (3 mJ, 10 Hz) of the Trident laser system, the autocorrelator was first aligned to obtain the second harmonic autocorrelation signal and a green laser diode (GD) was positioned along the direction of the autocorrelation signal within ±0.5 mrad of accuracy. At the target chamber side, using the low power cw alignment beam, the FROG system can be aligned up to the BBO crystal with the help of irises (I). After that the green diode (GD) is used to align the autocorrelation signal from the BBO crystal to the entrance slit of the imaging spectrometer IS2. The loosely focused autocorrelation signal along the spatial dimension is about 1.3 mm in size at the entrance slit of the imaging spectrometer IS2, which requires the green diode GD alignment accuracy to be better than ±0.87 mrad along the spatial dimension in order to point the autocorrelation signal into the spectrometer. This requirement is even more relaxed along the temporal dimension of the autocorrelation signal due to imaging. In this way, the whole device can be aligned before the actual high energy (80 J) shot.

III. MEASUREMENTS

Figures 2(a) and 2(b) show the measured FROG traces using the single shot SHG-FROG system for full energy (80 J) laser shots with no targets placed at TCC, representing typical variations in the incident laser pulses within the operational range of the Trident laser system. Figure 2(a) shows the FROG trace, which is symmetric in time and all the spectral components of the pulse arrive within ~1 ps time window. Also, the more oval-like shape of the FROG trace indicates the presence of a linear chirp (second order spectral phase) and a little bit of wings on the sides indicate the presence of a small pre- or postpulse with residual higher order spectral phase, referred to as nearly symmetric pulse (NSP). Figure 2(b) shows the FROG trace with slight asymmetry in time and the spectral components of the pulse arrive

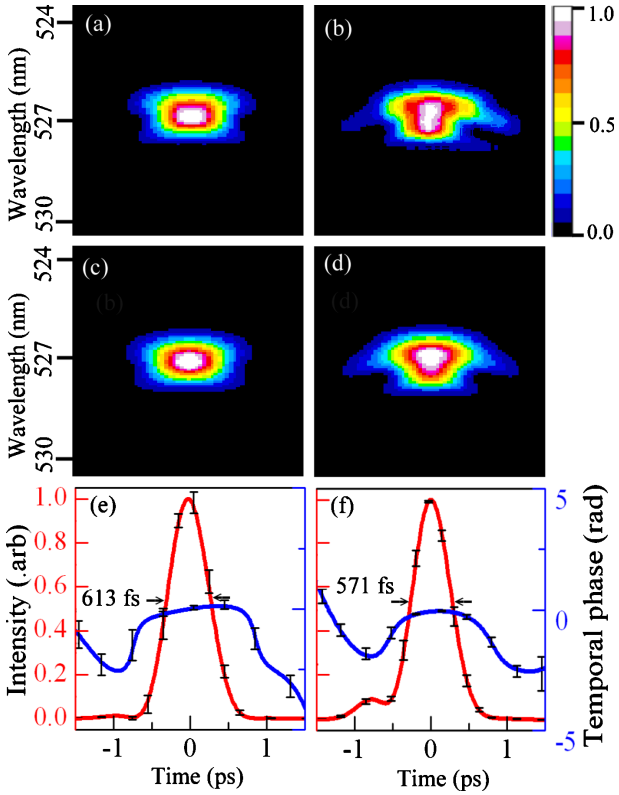

FIG. 2. (Color online) Measured FROG traces for (a) NSP and (b) ASP. Also shown on the right is the used linear-16 color scheme for the FROG traces. Reconstructed FROG traces from the inversion algorithm for (c) NSP and (d) ASP. Retrieved temporal intensity (solid line) and temporal phase (solid line) for (e) NSP and (f) ASP. The FWHM duration is 613 fs for (e) and 571 fs for (f).

within nearly 2 ps time window with significant wings on the sides. Also, the wings of the FROG trace indicate the presence of a large pre- or postpulse with significant residual higher order spectral phase, referred to as asymmetric pulse (ASP).

Figures 3(a) and 3(b) show the measured autocorrelation signal (dashed line) for NSP and ASP with FWHM durations of 817 and 858 fs, respectively. The autocorrelation signal looks symmetric for NSP, whereas for ASP we see a slight asymmetry at the foot of the pulse due to spatial nonuniformity in the beam profile. From the autocorrelation measurements, we see that the pulse duration for NSP is shorter than that of ASP and the foot of the autocorrelation signal for ASP falls off slower than NSP. Figures 3(c) and 3(d) show the measured spectrum of the laser pulse (dashed line) for NSP and ASP with spectral FWHM of 3 and 2.5 nm, respectively. For both the NSP and ASP, the shape of the spectrum looks nearly the same, except the 0.5 nm difference in their spectral FWHM.

IV. FROG INVERSION ALGORITHM

To begin, the measured FROG trace is resampled to meet the reciprocal Fourier transform requirement in both the temporal and spectral domains.[8] We use a "256×256" array size for the FROG trace in the FROG inversion

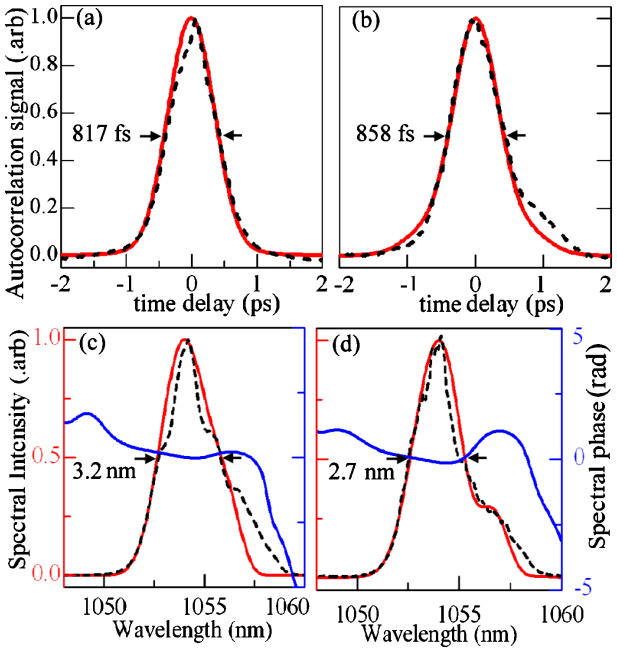

FIG. 3. (Color online) Autocorrelation signal calculated from pulse retrieved from FROG trace (solid line) and from measurement (short dash line) for (a) NSP and (b) ASP. Also shown are retrieved spectrums from FROG trace (solid line), from measurement (short dash line) and retrieved spectral phase from FROG trace (solid line) for (c) NSP and (d) ASP.

algorithm. After resampling the measured FROG trace, the FWHM of time and frequency signal in the FROG trace is roughly contained within an array size of "11×11." The inversion algorithm for retrieving pulse information from the measured FROG traces is based on the principal component generalized projection algorithm (PCGPA),[11] which is a two-dimensional iterative phase retrieval algorithm. The algorithm proceeds by generating a FROG trace using an initial random guess of the pulse and the gate and then replacing the magnitude of the generated FROG trace with that of the measured FROG trace while keeping the phase of the generated FROG trace unchanged. A new and improved guess of the pulse and gate pair can be obtained from this modified FROG trace via singular value decomposition (SVD). For an "$N\times N$" size FROG trace, the SVD produces "N" singular values and their corresponding pulse and gate pairs. The pulse (Pt) and gate (Gt) pair with the highest singular value is used as the input for the next iteration in the algorithm and the pair is forced to converge for SHG-FROG by constructing an outer product (O) as $O=[Pt^{*}Gt^{T}]+[\mathrm{conj}(Gt)^{*}\mathrm{conj}(Pt^{T})]$. Rotating the rows of the outer product gives the time-domain FROG, which can be Fourier transformed to give the FROG trace. The iteration continues until the FROG error between the measured (F) and reconstructed FROG trace (Fr) is minimized, while the FROG error is defined as $G=1/N[\Sigma(F-\alpha Fr)^2]^{1/2}$, where "$\alpha$" is a normalization parameter. A much faster convergence than SVD can be obtained by using the power method given as $Pt^{n}=OO^{T}\times Pt^{n-1}$ and $Gt^{n}=O^{T}O\times Gt^{n-1}$ for the next best guess of the pulse and gate pair. Generally, within a few iterations a good approximation of the pulse is obtained, while the algorithm converges in less than a minute for a typical processor speed.

V. RESULTS AND DISCUSSION

Figures 2(c) and 2(d) show the reconstructed FROG traces using the inversion algorithm and Figs. 2(e) and 2(f) show the retrieved temporal pulse shapes (solid line) and temporal phases (solid line) for the NSP and ASP, respectively. The FROG errors are 0.0039 and 0.0084 and the time-bandwidth products are 0.53 and 0.41 for the NSP and ASP, respectively. Representative error bars for the pulse shape and temporal phase measurements shown in Figs. 2(e) and 2(f) are obtained using the boot-strap method.[8] For NSP, the retrieved pulse has FWHM duration of 613 fs with a 1% pre- or postpulse at 1 ps away from the main peak. For ASP, the pulse has FWHM duration of 571 fs with a 10% pre- or postpulse at 800 fs away from the main peak. As well known, the SHG-FROG cannot differentiate between pre- and postpulse. In comparison with the autocorrelation measurements shown in Figs. 3(a) and 3(b), the FROG results show that the pulse duration for ASP is shorter than NSP. This shows that in such a large scale lasers pulse shape may be a more pertinent criteria than pulse duration. Figures 3(c) and 3(d) show the retrieved pulse spectrum from measured FROG trace (solid line) for NSP and ASP with FWHM of 3.2 and 2.7 nm, respectively, along with their corresponding spectral phases (solid line). For both the NSP and ASP, the spectral shape looks nearly the same except the 0.5 nm difference in their spectral FWHM. Also, in a 3 nm spectral window around 1057 nm the spectral phase for ASP has a larger curvature (higher order spectral phases) than NSP associated with changes of 0.5 and 2 rad, respectively. These differences in the spectral shape and phase lead to the observed significant pre- or postpulse for ASP than NSP shown in Figs. 2(e) and 2(f).

The retrieved FROG results are compared with independent measurements of spectrum and autocorrelation signal of the pulse to verify the FROG measurements. Figures 3(a) and 3(b) show the autocorrelation signal calculated (solid line) from the retrieved pulse from FROG measurements and the independently measured autocorrelation signal (dashed line) for NSP and ASP, respectively. For both the cases, the calculated and measured autocorrelation signals are in good agreement with each other. The difference between the retrieved and the measured autocorrelation signals in ASP at the foot of the pulse is due to a slight spatial nonuniformity in the input laser beam. Figures 3(c) and 3(d) show the pulse spectrum retrieved from the measured FROG trace (solid line) and that of an independent measurement (dashed line) for NSP and ASP, respectively. The overall agreement between the independently measured autocorrelation signal and spectrum and those retrieved from measured FROG traces supports the FROG measurements. With this single shot SHG-FROG system, we also observed the laser pulse shortening and shaping in the transmitted laser pulses when the laser interacts with diamondlike-carbon nanofoil targets. Those results will be explained in a separate publication.[4]

VI. CONCLUSION

To conclude, we have developed a single shot SHG based FROG system and a FROG inversion algorithm to characterize the laser pulses incident on and transmitted through nanofoils, relevant to the laser based electron/ion accelerations. The sampled laser beam is imaged onto the BBO crystal via a spatial filter to minimize diffraction effects. A pair of glass substrates is used to reduce the B-integral at high power. A prealigned green laser diode is used to align the autocorrelation signal from the BBO crystal to the entrance slit of the imaging spectrometer. The whole device can be completely aligned before the full energy (80 J) shot. We measured typical variation in the incident laser pulses from Trident laser system with the FWHM pulse durations from 571 to 613 fs. Going from longer to shorter pulse, the pulse develops a pre- or a postpulse that is 10% of the main peak. Finally, the FROG measurements are consistent with independent measurements of pulse spectrum and autocorrelation signal. The observed pulse variations show the relevance of developed pulse diagnostic for the general operation of high intense laser systems. Efforts are currently underway to use the diagnostic to optimize the incident pulse shape by collecting the entire low energy seed beam (10 Hz) at the end of the laser amplifier chain.

ACKNOWLEDGMENTS

We gratefully acknowledge the support of U.S. Department of Energy (DOE), U.S. Office of Fusion Energy Sciences (OFES), and DFG cluster of excellence Munich Center for Advanced Photonics for this work.

[1] B. M. Hegelich, B. J. Albright, J. Cobble, K. Flippo, S. Letzring, M. Paffett, H. Ruhl, J. Schreiber, R. K. Schulze, and J. C. Fernández, Nature (London) **439**, 441 (2006).
[2] W. P. Leemans, B. Nagler, A. J. Gonsalves, Cs. To'th, K. Nakamurai, C. G. R. Geddes, E. Esarey, C. B. Schroeder, and S.M. Hooker, Nat. Phys. **2**, 696 (2006).
[3] L. Yin, B. J. Albright, B. M. Hegelich, K. J. Bowers, K. A. Flippo, T. J. T. Kwan, and J. C. Fernández, Phys. Plasmas **14**, 056706 (2007).
[4] R. C. Shah, S. Palaniyappan, D. Jung, R. Johnson, T. Shimada, D. C. Gautier, S. Letzring, R. Hörlein, J. C. Fernandez, and B. M. Hegelich, "Self-induced relativistic transparency in ultra-intense laser nanofoil interactions" (unpublished).
[5] V. I. Eremin, A. V. Korzhimanov, and A. V. Kim, Phys. Plasmas **17**, 043102 (2010).
[6] C. Iaconis and I. A. Walmsley, Opt. Lett. **23**, 792 (1998).
[7] K. W. DeLong, R. Trebino, J. Hunter, and J. E. White, J. Opt. Soc. Am. B **11**, 2206 (1994).
[8] R. Trebino, *FROG: The Measurement of Ultrashort Laser Pulses* (Springer, New York, 2002).
[9] R. C. Shah, R. P. Johnson, T. Shimada, K. A. Flippo, J. C. Fernández, and B. M. Hegelich, Opt. Lett. **34**, 2273 (2009).
[10] A. E. Siegman, *Lasers* (University Science Books, Sausalito, California, 1986).
[11] D. J. Kane, J. Opt. Soc. Am. B **25**, A120 (2008).